29th International Congress on Sound and Vibration
The annual congress of the International Institute of Acoustics and Vibration (IIAV)
9–13 July 2023
ICSV29

EFFECT OF SPECTRAL SCATTERING ON RIJKE TUBE STABILIZATION BY A SIDE-BRANCH, NON-RESONATING DEVICE

Xingyu Zhang, Xue Han, Ying Hu, Tianyu Xu, and Lixi Huang

Lab for Aerodynamics and Acoustics, Zhejiang Institute of Research and Innovation, and Department of Mechanical Engineering, The University of Hong Kong, China

email: lixi.huang@hku.hk

Yumin Zhang

Lab for Aerodynamics and Acoustics, Zhejiang Institute of Research and Innovation, and School of Mechatronic Engineering and Automation, Foshan University, Foshan, China

Unstable sound waves are usually generated at the fundamental resonant frequency of the Rijke tube. In this study, we explore the design of a side-branch, non-resonating device in the simplest Rijke-tube configuration. The goal is to suppress thermoacoustic instability by spectral scattering towards different frequencies, which eliminates the in-phase feedback. Spectral scattering occurs when sound interacts with a device with time-varying properties, and time-variation is achieved by adding a MOSFET switch to the electromagnetic device which influences the acoustic impedance. The device is not active as it requires no sensing or control algorithm to operate despite the fact that there is an electrical current in the circuit. Numerical simulation reveals details of how the time-varying aspect of the device makes a crucial contribution towards the thermoacoustic instability control.

Keywords: Rijke tube, thermoacoustic instability control, spectral scattering

1. Introduction

Rijke tube serves as a useful tool for thermoacoustic problems [1] of combustion stability in ultra-lean fuel-mix environment. The unsteady heat release perturbations caused by turbulence in the flow or other thermodynamic factors generates sound waves, and when the combustion heat release pulsations are in phase with the generated sound waves, the pressure oscillations in the combustion chamber increase continuously and eventually reach a dangerous magnitude. Active control strategies [2-3] are well researched to deal with the instability, but its robustness is always hard to guarantee. Passive strategies are therefore preferred [4-5].

Rijke tube is a common platform to investigate control strategies of thermoacoustic instability. In our recent studies [6], we used a time-varying Shunt Electro-Magnetic Diaphragm (SEMD), as shown in Fig. 1, to achieve frequency modulation for normal incident sound waves. In this study, we apply the time-varying device [7] in a Rijke tube configuration. The key mechanism for thermoacoustic instability is the open-end of combustion chamber, which blocks the sound energy from escaping, and the reflected wave perturbates the flame forming a positive feedback loop hence instability. The aim of this study is to

demonstrate an alternative method of instability control, which is the conversion of the sound frequency away from the unstable mode to other frequencies, thus eliminating the in-phase feedback.

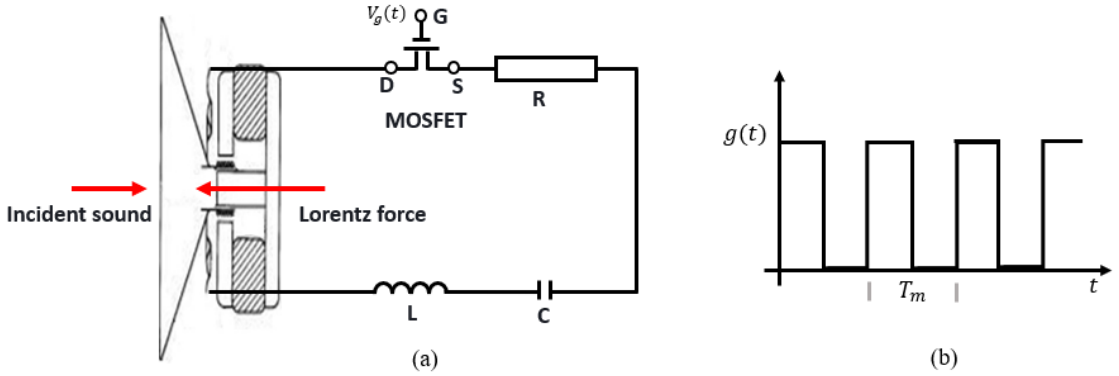

Figure 1: Schematic of the time-varying SEMD. (a) Time-varying SEMD realized by a shunted moving-coil loudspeaker cascading a MOSFET (metal–oxide–semiconductor field-effect transistor) unit, and (b) illustrates the MOSFET state function, g(t) = 1 for switch-on state and g(t) = 0 for switch-off state.

2. Theory

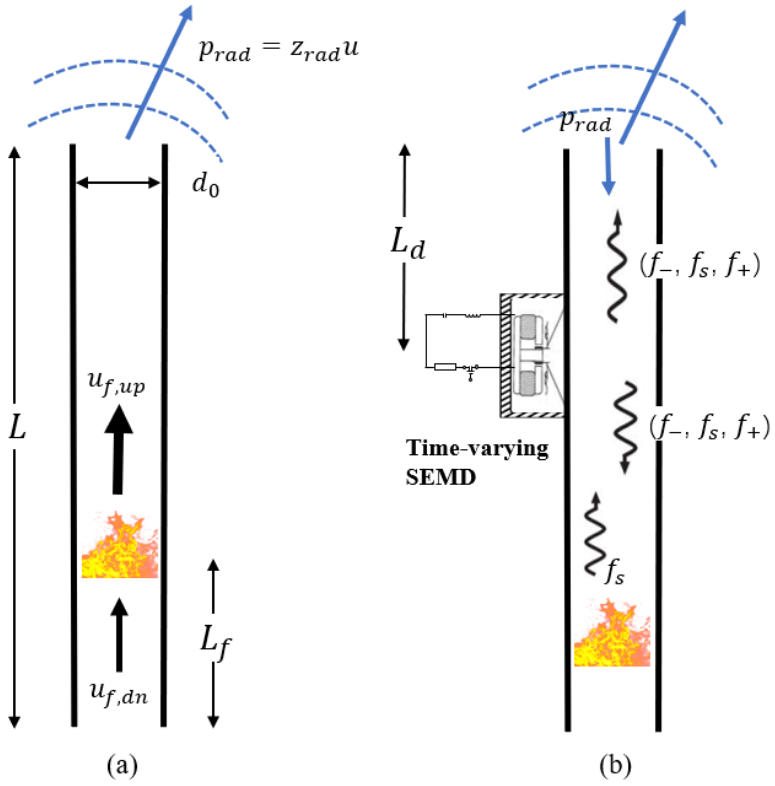

Figure 2: The configuration of this study. (a) defines the basic Rijke tube, and (b) illustrates the side-branch time-varying SEMD altering the incident wave frequency at a distance of $\boldsymbol{L_d}$ from the top end.

Figure 2 shows two configurations. The first is the Rijke tube without control and the second is with control by the side-branch time-varying SEMD. With the flow, once the strength of the flame reaches the critical value, the energy by heat release exceeds the energy loss by sound radiation, which triggers the instability. The generated sound is typically a harmonic sound, and its wavelength equals to twice of the tube length, or the sound with several isolated frequencies that are multiples of the former sound

frequency ($f_s = c_0/2L$). Our recent study [6] has experimentally demonstrated that we can convert the sound frequency of incident sound linearly. Typically, the new frequencies are equal to $f_s \pm nf_m$, where f_m is the modulation frequency by the MOSFET and $n = 1$ is the dominate order of modulation. For the sound of these new frequencies, no constructive coupling with the flame perturbation is considered.

In this realization, we use an electro-magnetic diaphragm shunted by an analogue circuit, illustrated in Fig. 1(a). The applied diaphragm serves as a sound absorber rather than a sound source. The two terminals of the diaphragm are connected by s shunt circuit only consisting of passive elements such as resistors, capacitors, and inductors. When the incident wave pushes the diaphragm, the coil of the diaphragm will cut the magnetic field behind, thus generating the electric current, and the voltage in the circle is determined by the electrical characteristics of both the diaphragm and elements wired into the circuit. The induced current through the moving coil causes a Lorentz force, and this force is against the pressure acting on the diaphragm surface, which means that the mechanical impedance of the diaphragm is affected by the electrical impedance of the circuit. Thus the circuit can be designed to get a desired mechanical performance of the diaphragm.

The method to achieve the time-varying device is to wire a MOSFET into the circuit to dynamically connect or disconnect the shunt circuit, illustrated in Fig. 1(a). The switching action of this transistor is preprogramed. Thus, this time-varying device is passive. There are three terminals on a MOSFET, Gate, Source, and Drain. The transistor's on-resistance is controlled by the voltage supplied at the "Gate" terminal. If the voltage exceeds a threshold, the effective resistance between the other two terminals is very small, e.g., $10\text{m}\Omega$, which can be regarded as the switch-on state g(t) = 1, otherwise it is very large, e.g., 4000Ω, which can be regarded as the switch-0ff state g(t) = 0. The switching occurs at the nanosecond level, thus there is no need to consider the transition state. It is feasible to have frequent control of the change in the two states of the transistor, as shown in Fig. 1(b). Therefore, the impedance of the diaphragm can change over time with MOSFET. In addition, both the characteristics of impedance and the variation rate can be designed according to the design task.

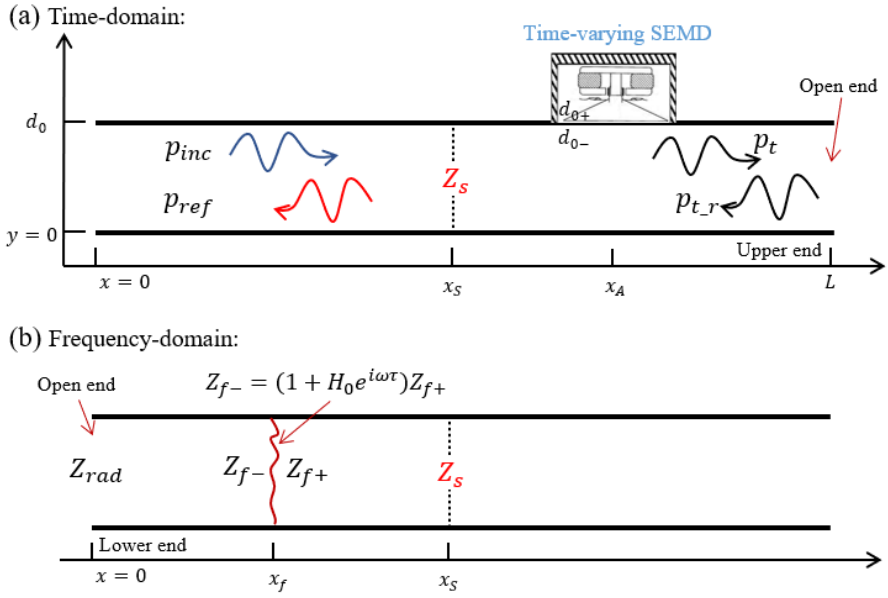

Figure 3: The configuration of the numerical simulation. (a) is first simulated in the time-domain, and then the result of the impedance at the cross-section $x = x_s$ can be used by the frequency domain analysis (b) for further thermoacoustic instability analysis.

For the numerical calculation, a commercial FEM software COMSOL Multiphysics (https//www.comsol.com/comsol-multiphysics) is used. As shown in Fig. 3 (a), the Rijke tube with a

side-branch time-varying SEMD is modelled using the Pressure Acoustics, Transient interface. The boundary conditions for the time-domain numerical calculations are set as the following.

The motion of the diaphragm is driven by the force of the total pressure difference acting on the diaphragm surface $\int (p_{d_{0-}} - p_{d_{0+}})\mathrm{d}A$, and it is controlled by the following governing equations.

$$M\frac{\mathrm{d}v}{\mathrm{d}t} + Dv + K\eta + BlI = \int (p_{d_{0-}} - p_{d_{0+}})\mathrm{d}A,\ v = \frac{\mathrm{d}\eta}{\mathrm{d}t}. \tag{1}$$

where η is the displacement, M, D, and K are the dynamic mass, damping, and stiffness of the suspended diaphragm, respectively, B is the magnetic flux density, l is the effective length of the coil cutting the magnetic field, and I is the electric current in the shunt circuit. The Ampere force in the above equation is controlled by the following governing equation for the shunt circuit.

$$L\frac{\mathrm{d}I}{\mathrm{d}t} + R(t)I + \frac{q}{C} = Blv,\ I = \frac{\mathrm{d}q}{\mathrm{d}t},\ R(t) = R_{on} + R_{off}[1 - g(t)]. \tag{2}$$

where q is the electrical charge, L, R, and C are the total inductance, resistance, and capacitance of the shunt circuit containing the electric impedance of the coil and the wired elements, respectively, R_{on} and R_{off} are the resistances corresponding to the two states of MOSFET, respectively. We apply a parameter sweep to make the governing equations to toggle between switch-on and switch-off. The coupled Eqs. (1) and (2) are solved for the displacement, and then applied on the surface of the diaphragm.

A "background pressure field" in Comsol and perfectly matched layer are applied on the left-hand side of the tube to provide an incident wave f_s and no-reflection boundary condition. At the right-hand side of the tube, a large circular computational domain is set to warp out the upper end of the tube and an additional perfectly matched layer is set on the outer layer of the said circular domain to achieve an open-end boundary condition.

Due to the special property of the Rijke tube, only the amplitude ratio p_{ref}/p_{inc} at the resonance frequency is of concern, while other reflections can be ignored. Once the amplitude ratio of the sound-emitting frequency is obtained, the impedance at the cross-section $x = x_s$ can be calculated as

$$Z_s = \frac{p_{inc}e^{-ikx_s} + p_{ref}e^{ikx_s}}{p_{inc}e^{-ikx_s} - p_{ref}e^{ikx_s}}. \tag{3}$$

where p_{inc} is the given pressure amplitude of the incident wave, p_{ref} is the calculated complex pressure amplitude of the reflected wave, and $k = 2\pi f_s/c_0$.

The obtained impedance can then be carried over to the same position in the frequency-domain calculation, as shown in Fig. 3(b). With the upper and lower impedances (Z_{rad} and Z_s), we can use the impedance transfer function to get the impedance above and below the flame (Z_{f+} and Z_{f-}), and then use the heat transfer function $Z_{f-} = (1 + H_0 e^{i\omega\tau})Z_{f+}$ [8] for further thermoacoustic instability analysis. The impedance transfer function and calculation procedure are introduced in our previous work [9]. Due to the page limitation, this paper only describes the performance of the side-branch, time-varying device, and the thermoacoustic instability analysis can be conducted by the procedure described in [9].

3. Results

The proposed calculation procedure is applied to a Rijke tube with a diameter of d_0 = 2 inches and a length of L = 1 m. The resonance frequency is around $180\text{Hz} \approx c/2L$, thus the incident wave frequency analysed in the following is 180Hz, and the broadband performance will be given in the end. The location of the flame is at the lower quarter of the tube $L_f = 0.25L$, and the device is positioned at $L_d = 0.3L$ from the top open-end of the tube. The mechanical and electrical parameters of the SEMD are listed in Table 1.

Table 1: A set of typical mechanical and circuit parameters

D [Ns/m]	M [g]	K [N/m]	Bl [Tm]
0.648	5.7	1822	4.6
R [Ω]	C [uF]	L [mH]	f_m [Hz]
0.11	824.7	0.45	170

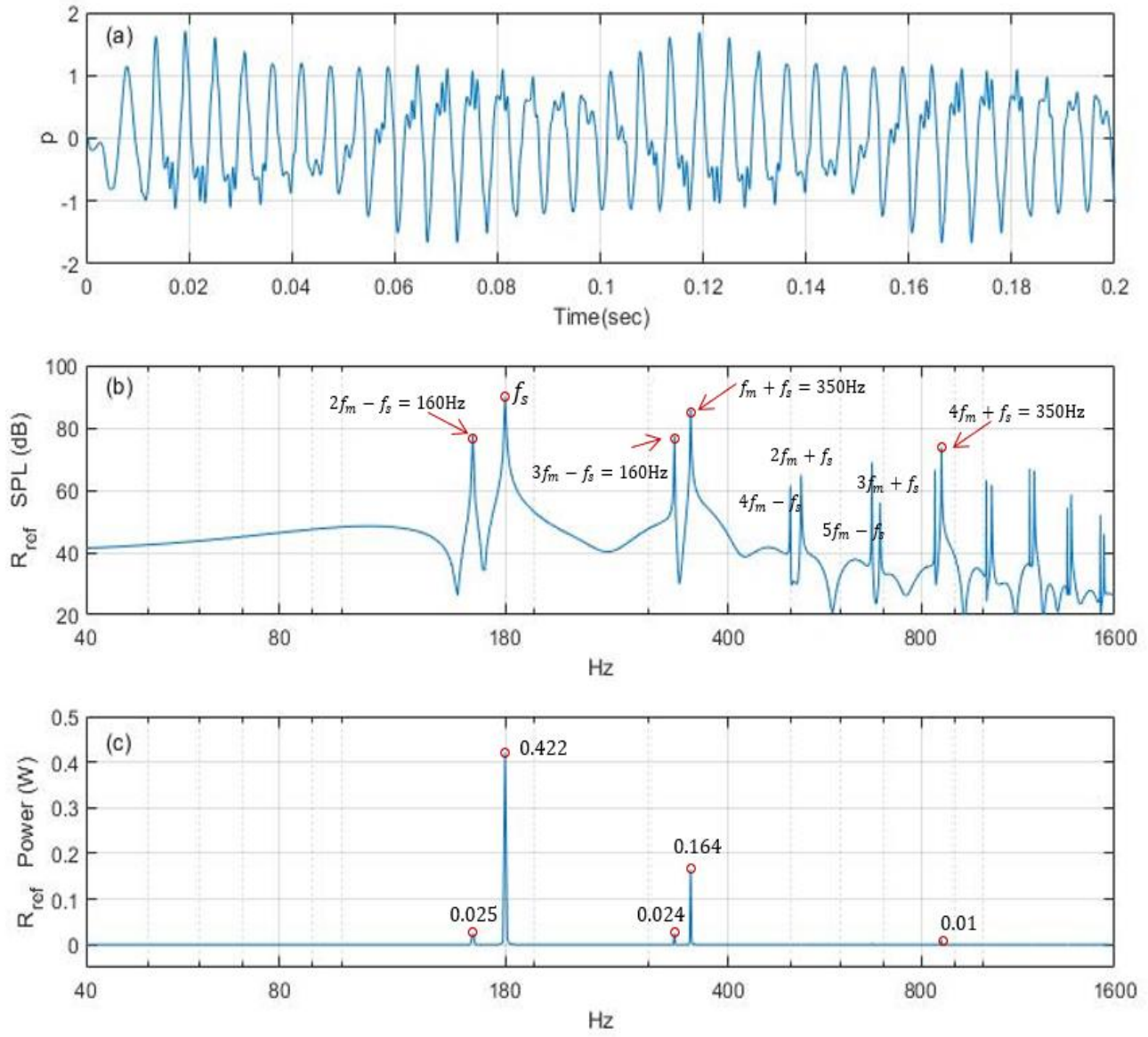

Figure 4: Time-domain results for the frequency modulation ($f_s = 180\text{Hz}, f_m = 170\text{Hz}$). (a) is the waveforms at the cross-section $x = x_s$; (b) is the sound pressure level spectra of the reflected wave R_{ref}. (c) is the normalized sound power of the reflected wave R_{ref}. The main components of the reflected waves are marked in (b) and (c).

Figure 4 shows the time domain numerical results. With the modulation, it seems that the sound waves are distorted and the modulated wave has new frequencies, as shown in Fig. 4(a). It's because that the acoustic impedance of the SEMD varies with time at the frequency of f_m. The diaphragm acts as a wave multiplier instead of a constant filter. A time-domain multiplier convolutes the sound at frequency

domain, which leads the linear frequency conversion effect. The incident wave hence is distorted and contains many new frequencies. The spectra of the modulated waves clearly demonstrate this point, which are shown in Fig. 4(b). There are significant portions of sound waves at other new frequencies in the spectra shown in Fig. 4(b), which validates the frequency conversion effect. Ideally, if the impedance of the SEMD changes in a sine pattern against time, we can only convert the incident sound wave to the difference and summation frequencies. However, the MOSFET in SEMD behaves like a square function against time, which is a combination of many Fourier series components. The impedance of the SEMD, therefore, also varies with time like a square wave which finally produces many lines for the modulated wave. As we have described above, the new frequencies are equal to $f_s \pm nf_m$, and the main five components are marked with the red circles in Figs. 4(b) and 4(c).

For the Rijke tube, the modulated waves also interact with the flame, however, it will not accumulate energy as we know that integrating the product of two sine waves of different frequencies leads to zero over a long time. With such consideration, energy of the sound waves of new frequencies is equivalent to being absorbed. What really matters is the sound power of the reflected wave and how much of it is being absorbed including the frequency conversion effect, which is shown in Fig. 4(c). The reflected sound power is normalized by that of the incident sound wave. It shows that the intensity of the reflected wave at the original frequency accounts for 0.422 and the sound wave at the first-order summation frequency ($f_s + f_m = 350$Hz) accounts for 0.164. This result means 57.8% of the reflected energy is eliminated, which can significantly increase the critical value of the Rijke tube at 180Hz. The broadband performance of this time-varying device is shown in Fig. 5.

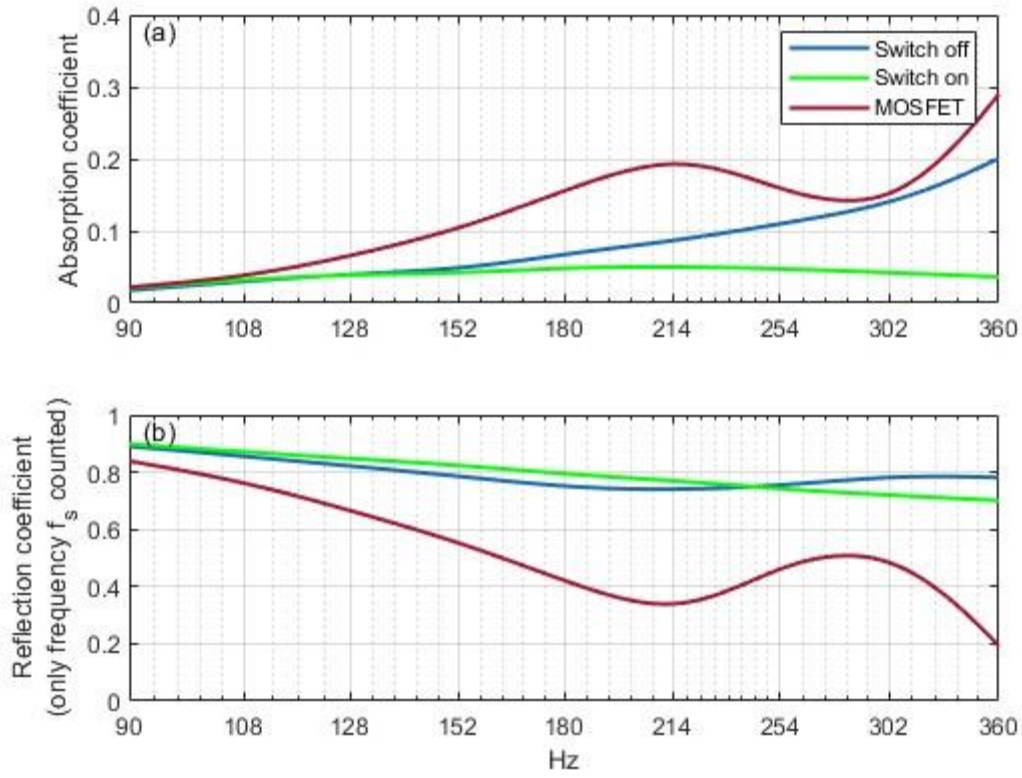

Figure 5: Energy analysis of the SEMD with different states, switch-on, switch-off and the MOSFET state. The horizontal coordinate represents the incident wave frequency f_s, the mechanical and electrical parameters of SEMD are fixed including the modulation frequency f_m. (a) Absorption coefficient and (b) reflection coefficient of the side-branch, time-varying SEMD.

Figure 5 shows the performance of the same time-varying SEMD with different incident waves over two octave bands. When the state is switch-off, there is no current inside the circuit and the SMED is a pure mechanical diaphragm, while the state is switch-on, there is a current in the circuit and the resulting Lorentz force will prevent the vibration. Therefore, the switch-off state will absorb more energy. With MOSFET, the absorption coefficient includes the absorbed sound energy at the incident and modulated frequencies, thus making the situation inside the tube much more complicated. The incident wave will be partially absorbed and converted first, and then the converted wave will be absorbed and converted again, resulting in a high absorption coefficient, as shown in Fig. 5(a).

Figure 5(b) shows the reflection coefficient. Note that only the reflected coefficient is not equal to 1 minus the absorption coefficient. The incident energy is split into three parts, the absorbed, the reflected and the open-end radiated. For both the switch-off and switch-on states, the reflected sound power is all counted, because their sound waves have only one frequency f_s, and this differs from the case when we apply the MOSFET. With a MOSFET, we can ignore a large percentage of the converted waves that will not cause feedback, while neither of the other two states can change the wave frequency. Therefore, the time-varying SEMD has a low reflection coefficient and a good performance for the Rijke tube.

Figure 5 shows the broadband effect of this side-branch, time-varying SEMD. The above results focus on the resonant frequency (180Hz) for a pure Rijke tube with a length of 1m. But in the real application, the resonance frequency will change after the installation of this device. The results in Fig. 5 show that even if the resonant frequency shifts, the time-varying device can still effectively suppress the instability over two octave bands.

4. Concluding discussions

In this work, we introduced a time-varying SEMD which captures the known features of the Rijke tube and provides a new strategy to address the thermoacoustic instability. Contrary to common approaches for dealing with thermoacoustic instability, absorption or phase variations, this device directly converts the incident wave to different frequencies to disrupt the closed feedback loop. For the example given, the device has a 0.422 reflection coefficient at the Rijke resonance frequency and a good broadband performance over two octaves. Future studies will focus on further improving the conversion efficiency of the side-branch time-varying SEMD and the experiments.

REFERENCES

1 Lord Rayleigh. The explanation of certain acoustical phenomena, Nature 18 (455): 319–321 (1878).

2 Heckl, M. Active control of the noise from a Rijke tube, J. Sound Vib. 124: 117–133 (1988).

3 Dowling, A. P. and Morgans, A.S. Feedback control of combustion oscillations, Annu. Rev. Fluid Mech. 37: 151–182 (2005).

4 Zhao, D., Morgans, A.S. and Dowling, A. P. Tuned passive control of acoustic damping of perforated liners, AIAA J. 49 (4): 725–734 (2011).

5 Zhang, Y. and Huang, L. Electroacoustic control of Rijke tube instability, J. Sound Vib. 409: 131-144 (2017).

6 Zhang, Y., Wu, K., Wang, C. and Huang, L. Towards altering sound frequency at will by a linear meta-layer with time-varying and quantized properties, Commun. Phys. 220 (2021).

7 Huang, L., Wu, K., Xue, H. and Zhang, Y. Mechanism of low frequency spectral scattering by a side-branch electromagnetic device with switching shunt, J. Sound Vib. 545 (2023).

8 A.P. Dowling, The calculation of thermoacoustic oscillations, J. Sound Vib. 180: 557–581 (1995).

9 Zhang, X., Wu, K., Zhang, Y. and Huang, L. Sidebranch bypass for thermoacoustic sound, ICSV27 (2021).